Broj rada: 4.2
DOI: 10.65156/wws.sjdp.si.018

UTICAJ TIG PRETAPANJA AKTIVIRANOG NANOČESTIČNIM FLUKSEVIMA NA BRUŠENE PWAAM AL–CU–SI DEPOZITE PRIMENOM JEDNOSMERNE STRUJE

EFFECT OF NANOPARTICLE-BASED ACTIVATED TIG REMELTING ON GROUND PWAAM AL–CU–SI ALLOY DEPOSITS USING DC CURRENT

Albert Hauck[1] 0009-0003-8055-3886, Norbert Enzinger[2], 0000-0003-0051-9518, Miroslav Dramicanin[1] 0000-0002-9079-0864, Dragan Rajnovic[1] 0000-0002-5303-4402, Matthias Moschinger[2] 0000-0001-8272-3904, Fernando Warchomicka[2] 0000-0002-4909-8657, Milan Pecanac[1] 0000-0002-8016-9986, Sebastian Balos[1] 0000-0002-3828-8500

1 Department of Production Engineering, Faculty of Technical Sciences, University of Novi Sad, Trg Dositeja Obradovica 6, 21102 Novi Sad, Serbia

2 Institute of Materials Science, Joining and Forming, Graz University of Technology, Kopernikusgasse 24, 8010 Graz, Austria

E-mail: albert.hauck@uns.ac.rs

Rezime: Plazma aditivna proizvodnja (PWAAM) omogućava izradu aluminijumskih in-situ legura primenom više dodatnih žica. Međutim, usled različitog ponašanja legirajućih elemenata pri topljenju, može doći do nepotpunog rastvaranja, odnosno pojave zaostalih oblasti bogatih bakrom i mikrostrukturne nehomogenosti. U ovom radu su brušeni PWAAM depoziti legure Al–Cu–Si pretapani primenom konvencionalnog TIG pretapanja i aktiviranog TIG pretapanja pri jačini jednosmerne struje od 173 A. Cilj rada bio je ispitivanje uticaja aktivirajućih flukseva na bazi nanočestica na geometriju pretopljene zone, mikrostrukturu i mikrotvrdoću. Upoređena su tri fluksa, na bazi nanočestica 20 nm TiO_2, 40 nm SiO_2 i 5 nm SiO_2, sa pretapanjem bez fluksa. Rezultati su pokazali da aktivirajući fluks utiče na dubinu uvara, širinu pretopljene zone, a samim tim i na površinu pretopljene oblasti. Fluks na bazi 40 nm SiO_2 doveo je do formiranja najveće pretopljene zone, dok je fluks na bazi 20 nm TiO_2 omogućio najizraženije usitnjavanje mikrostrukture. Fluks na bazi 5 nm SiO_2 takođe je povećao površinu pretopljene zone u poređenju sa pretapanjem bez fluksa, iako su lokalno uočene zaostale oblasti bogate bakrom. Svi ispitivani uzorci pokazali su relativno nisku poroznost. Merenja mikrotvrdoće pokazala su povećane vrednosti u okviru pretopljenih oblasti, pri čemu je najveća tvrdoća izmerena kod uzorka pretapanog uz primenu TiO_2 fluksa. Dobijeni rezultati ukazuju da se aktivirano TIG pretapanje jednosmernom strujom može primeniti za modifikaciju geometrije pretopljene zone i poboljšanje lokalnih mikrostrukturnih karakteristika i mikrotvrdoće brušenih PWAAM Al–Cu–Si depozita.

Ključne reči: plazma aditivna proizvodnja, aktivirano TIG pretapanje, fluks na bazi nanočestica, geometrija pretopljene zone, mikrotvrdoća

Abstract: Plasma wire arc additive manufacturing (PWAAM) enables the production of aluminium based in-situ alloys using multiple wire feeds, but with incomplete solution, that is, retained Cu rich regions and microstructural heterogeneity may occur due to the different melting behaviour of the alloying elements. In this study, ground PWAAM Al–Cu–Si alloy

deposits were remelted using conventional TIG remelting and activated TIG remelting at a current of 173 A. The aim was to investigate the influence of nanoparticle based activating fluxes on remelted zone geometry, microstructure and microhardness. Three fluxes, based on 20 nm TiO_2, 40 nm SiO_2 and 5 nm SiO_2 nanoparticles, were compared with flux free TIG remelting. The results showed that the activating flux affected penetration depth, remelted width and thereby remelted area. The 40 nm SiO_2 flux produced the largest remelted zone, while the 20 nm TiO_2 flux resulted in the most pronounced microstructural refinement. The 5 nm SiO_2 flux also increased the remelted area compared with flux free remelting, although retained Cu-rich particles were still observed locally. All investigated ground specimens exhibited relatively low porosity. Microhardness measurements showed increased values within the remelted regions, with the highest hardness obtained in the TiO_2-assisted specimen. The results indicate that DC activated TIG remelting of ground PWAAM Al–Cu–Si deposits can be used to modify remelted zone geometry and improve local microstructural and hardness characteristics.
Key words: plasma wire arc additive manufacturing, activated TIG, nanoparticle-based flux, remelted zone geometry, microhardness

Keywords: plasma wire arc additive manufacturing, activated TIG, nanoparticle-based flux, remelted zone geometry, dendritic microstructure, microhardness

1. INTRODUCTION

Wire arc additive manufacturing (WAAM) is a directed energy deposition process in which an electric arc is used to melt and deposit metallic wire feedstock layer by layer. Compared with powder-based additive manufacturing processes, WAAM offers high deposition rates, efficient material utilization and the possibility of using commercially available welding wires, making it particularly suitable for the production and repair of large metallic components [1]. Depending on the heat source, WAAM can be based on metal inert gas, tungsten inert gas or plasma arc welding. When a plasma arc is used as the heat source, the process is commonly referred to as plasma wire arc additive manufacturing (PWAAM). Due to the constricted plasma arc, PWAAM provides high energy density, stable heat input and efficient melting, which makes it suitable for the deposition of complex alloys and for in-situ alloying using multiple wire feeds [2,3]. Dual wire PWAAM is especially interesting for the production of alloys that are difficult or unavailable as conventional wire feedstock. By adjusting the feed rates of two different wires, the final chemical composition of the deposited material can be controlled during processing. This approach is relevant for Al–Cu–Si alloys, which have attracted attention due to the possibility of obtaining multiphase eutectic or near eutectic microstructures with high strength and useful ductility. Previous studies on cast Al–Cu–Si alloys reported promising combinations of strength and plasticity, related to microstructures consisting of α-Al, Al_2Cu and Si containing eutectic constituents [4-6]. However, the transfer of such alloy concepts to wire-based additive manufacturing is not straightforward. In dual wire in-situ alloying, the wires may differ significantly in melting temperature, thermal conductivity, density, wetting behaviour and chemical composition. These differences can lead to incomplete mixing, local variations in dilution and the formation of retained Cu rich regions in the deposited material. As a result, the PWAAM deposit may exhibit microstructural heterogeneity, non-uniform phase distribution and local changes in hardness [7-9]. For Al–Cu–Si deposits, this is particularly important because copper segregation and retained Cu rich particles can strongly influence the final microstructure and mechanical response. One possible post-processing approach for reducing local heterogeneity is remelting of the deposited surface layer. Tungsten inert gas (TIG) remelting is a simple and industrially applicable method for modifying the near-surface region of metallic materials. In activated TIG (ATIG) processing, an activating flux is applied to the

surface before remelting. The flux can influence arc behaviour, heat transfer and molten pool flow, often resulting in modified penetration depth and remelted zone geometry. In aluminium alloys, the surface oxide layer also plays an important role, since Al_2O_3 can affect arc coupling and heat transfer. Therefore, surface preparation before remelting may influence the interaction between the arc, flux and deposited material [10,11]. In this study, ground PWAAM Al–Cu–Si alloy deposits were remelted using conventional TIG and activated TIG processing with direct current at 173 A. The surface of the deposits was ground prior to remelting in order to remove the oxide layer and provide more uniform interaction between the arc and the material. Three nanoparticle based activating fluxes were investigated, based on 20 nm TiO_2, 40 nm SiO_2 and 5 nm SiO_2 particles, and compared with flux free TIG remelting. The aim of the work was to determine the influence of nanoparticle based flux composition on remelted zone geometry, microstructure and microhardness of ground PWAAM Al–Cu–Si deposits.

2. EXPERIMENTAL PART

2.1. PWAAM deposition of Al–Cu–Si alloy deposits

The Al–Cu–Si alloy deposits used in this study were produced by plasma wire arc additive manufacturing (PWAAM). An AW1050 aluminium plate with dimensions of 100 mm × 200 mm × 5 mm was used as the substrate material. Prior to deposition, the surface area intended for building the deposit was cleaned using a transferred plasma arc in order to remove surface oxides and improve the adhesion of the first deposited layer. The PWAAM process was performed using an SBI-M3DP-SL machine equipped with a PWM-450 plasma torch and an Ø8 mm plasma nozzle. During deposition, the distance between the plasma nozzle and the deposit surface was kept constant at 10 mm. Dual wire feeding was applied directly into the plasma arc, opposite to the welding direction, in order to enable in-situ alloying within the molten pool. The wires used were MA-4043, corresponding to an AlSi5-type filler wire, and ML-CuAl8. The wire feed rates were adjusted to 80 mm/s for MA-4043 and 16 mm/s for ML-CuAl8, with the aim of obtaining an AlCu15Si4-type composition in the deposited material. The main parameters used in substrate cleaning and PWAAM deposition are given in Table 1.

Table 1. PWAAM parameters used for substrate cleaning and deposition

Process step	Current [A]	Frequency [Hz]	Balance -/+	Voltage [V]	Travel speed [mm/s]	Plasma gas [l/min]	Shielding gas [l/min]
Cleaning	100	60	70/30	20	10	1	13
Deposition	260	60	70/30	28	4	1	13

After deposition, the PWAAM structures were milled to obtain a more uniform surface suitable for subsequent TIG and activated TIG remelting. Before remelting, the investigated specimens were additionally ground using P1000 abrasive paper. The deposition path plan and the prepared deposit surface are shown in Figure 1.

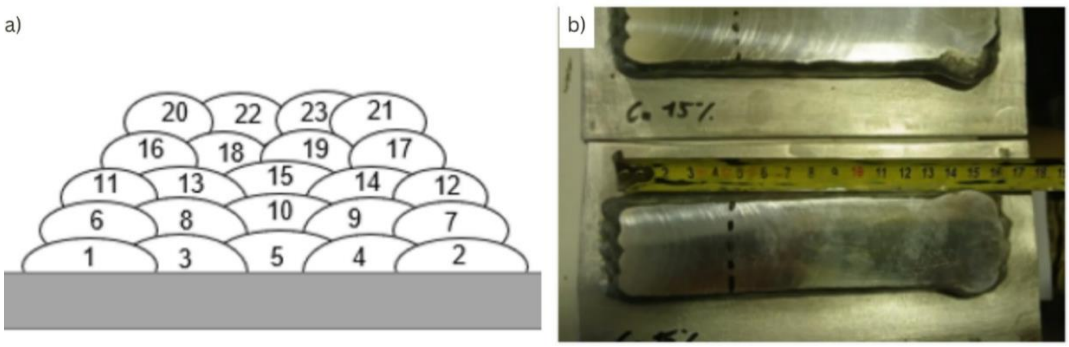


Figure 1. PWAAM Al–Cu–Si deposit preparation: a) deposition path plan; b) deposit surface after milling/grinding and before TIG/ATIG remelting.

2.2. TIG and activated TIG remelting

The ground PWAAM deposits were remelted using conventional tungsten inert gas (TIG) remelting and activated TIG (ATIG) remelting. The purpose of remelting was to modify the surface layer of the PWAAM deposit, reduce local microstructural heterogeneity and promote the dissolution of retained Cu-rich regions into the aluminium matrix. Remelting was performed using a Lorch HandyTIG welding device. A 2% thoriated tungsten electrode with a diameter of 2.4 mm was used. For direct current remelting, the electrode tip was sharpened to an angle of 60°. The electrode protruded 6 mm from an Ø12.7 mm nozzle, while the distance between the electrode tip and the deposit surface was kept constant at 2 mm. The remelting process was carried out using a Lorch Trac WL welding tractor, which enabled a constant travel speed of 40 mm/min. Four 100 mm long remelting passes were produced on each deposit, with cooling to room temperature between passes. The remelting experiments were performed on ground PWAAM Al–Cu–Si deposits using 173 A direct current. Three nanoparticle-based activating fluxes were investigated and compared with conventional flux-free TIG remelting. The fluxes were prepared using sodium silicate (Na_2SiO_3) as the solvent and oxide nanoparticles as active components. The investigated nanoparticles were 20 nm TiO_2, 40 nm SiO_2 and 5 nm SiO_2. The flux components were weighed using an analytical balance and mixed with the solvent using a magnetic stirrer for 10 min.

Table 2. Investigated ground specimens remelted using 173 A DC current

Specimen designation	Current type	Current [A]	Flux
D173-0G	DC	173	Without flux
D173-TG	DC	173	20 nm TiO_2
D173-S4G	DC	173	40 nm SiO_2
D173-S5G	DC	173	5 nm SiO_2

2.3. Characterization

Metallographic preparation was performed in order to determine the geometry of the remelted zones and to analyse the resulting microstructure. Cross sections were cut at approximately two thirds of the remelted pass length, measured from the beginning of the pass. The samples were cut using a SiC cutting wheel with cooling, followed by cold mounting in a PMMA polymer matrix. The mounted specimens were ground using SiC abrasive papers from P320 to P2000 and polished using a 40 nm colloidal silica suspension. The macrogeometry of the remelted zones was analysed by light microscopy using a Leitz Orthoplan microscope. The obtained

images were stitched and aligned using Hugin software, while the remelted zone area was determined using Fiji image processing software. The main geometrical parameters considered in this study were penetration depth, remelted zone width, reinforcement height and total remelted area. Microstructural analysis of selected specimens was performed using a Tescan Mira 3 field-emission scanning electron microscope (FE-SEM), together with energy-dispersive spectroscopy (EDS). SEM and EDS analyses were used to observe dendritic morphology, Cu-rich regions and local chemical homogeneity within the remelted zones. Microhardness measurements were carried out using a Wilson Tukon 1102 microhardness tester with a load of 0.5 kg (HV0.5). Measurements were performed in two directions. The first profile was measured horizontally, 2 mm below the specimen surface, with an indentation spacing of 1 mm. The second profile was measured vertically from the remelted surface towards the melt line and into the PWAAM base material. This enabled comparison between the remelted zone and the underlying additively manufactured material.

3. RESULTS AND DISCUSSION

3.1. Remelted zone geometry

The macrosections of the ground PWAAM Al–Cu–Si deposits remelted using 173 A DC current are shown in Figure 2. The application of nanoparticle based activating fluxes clearly affected the geometry of the remelted zone. Compared with flux free TIG remelting, the use of activating fluxes increased the remelted area, although the effect depended strongly on the flux composition. The largest remelted zone was obtained for the specimen treated with 40 nm SiO_2 flux, indicating the most pronounced influence on penetration depth and remelted zone width. The specimen treated with 5 nm SiO_2 also exhibited an increased remelted area compared with flux free remelting, while the TiO_2 assisted specimen produced a more moderate remelted zone. All investigated specimens exhibited relatively low porosity. However, local Cu rich regions were still observed in some cases. In the specimen treated with 40 nm SiO_2 flux, retained Cu rich material was mainly located near the melt line, while in the specimen treated with 5 nm SiO_2 flux, local Cu rich particles were observed within the remelted region. This indicates that the applied remelting parameters were generally effective in modifying the PWAAM deposit, but complete dissolution of retained Cu rich regions was not achieved in all flux conditions.

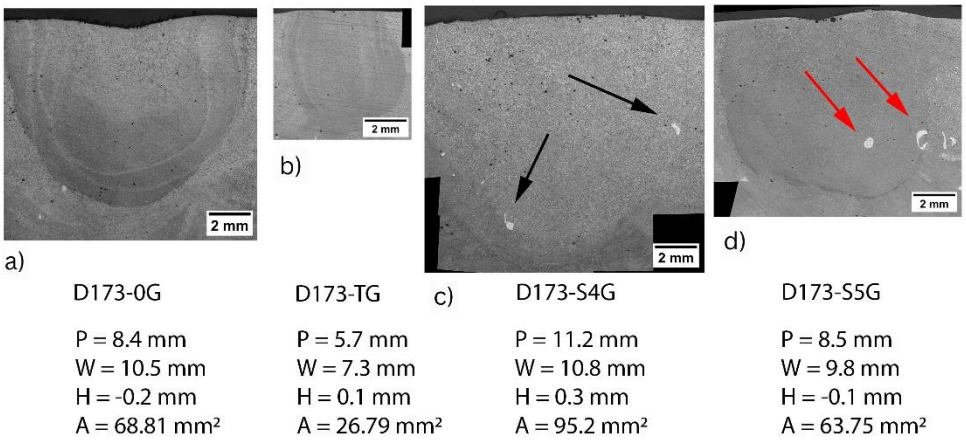


Figure 2. Macrosections of ground PWAAM Al–Cu–Si deposits remelted using 173 A DC current: (a) D173-0G, flux-free TIG remelting; (b) D173-TG, 20 nm TiO_2 flux; (c) D173-S4G, 40 nm SiO_2 flux; (d) D173-S5G, 5 nm SiO_2 flux.

3.2. Microstructural characteristics

Representative micrographs of ground DC ATIG remelted PWAAM Al–Cu–Si deposits treated with the investigated nanoparticle based fluxes are shown in Figure 3. The most pronounced refinement was observed in the specimen treated with 20 nm TiO_2 flux, where finer dendrites and smaller dendritic colonies were obtained. This suggests that TiO_2 particles promoted heterogeneous nucleation and limited dendrite growth during solidification, which is consistent with the relationship between dendrite spacing and cooling conditions [12]. The specimen treated with 40 nm SiO_2 also exhibited a refined dendritic structure, although the refinement was less pronounced than in the TiO_2 assisted specimen. In contrast, the 5 nm SiO_2 flux resulted in comparatively coarser dendritic features, which may be related to the stronger tendency of very small nanoparticles to agglomerate, thereby reducing their effective number of nucleation sites [13]. The flux free specimen showed the coarsest dendritic morphology among the investigated conditions. These observations indicate that the effect of the activating flux is not limited only to the geometry of the remelted zone, but also influences the solidification behaviour and resulting dendritic morphology. While 40 nm SiO_2 was more effective in increasing the remelted area, 20 nm TiO_2 had a stronger effect on microstructural refinement. This distinction is also reflected in the microhardness results.

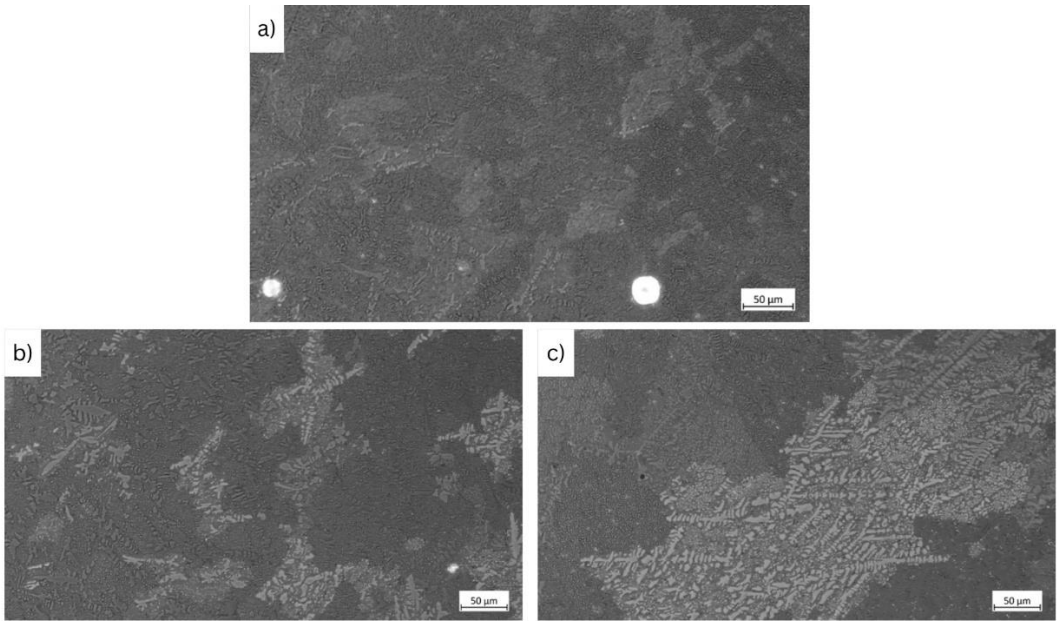


Figure 3. Microstructures of ground DC ATIG-remelted PWAAM Al–Cu–Si deposits treated with different nanoparticle-based fluxes: (a) D173-TG, 20 nm TiO_2; (b) D173-S4G, 40 nm SiO_2; (c) D173-S5G, 5 nm SiO_2.

3.3. Microhardness

The microhardness profiles measured in the horizontal and vertical directions are shown in Figure 4. Increased microhardness values were observed within the remelted zones, while lower values were measured in the surrounding PWAAM-deposited material. The shape of the microhardness profiles corresponded well with the macrogeometry of the remelted zones, confirming that the modified region can be clearly distinguished from the underlying deposit. The highest microhardness values were obtained in the TiO_2 assisted specimen, followed by the

specimens treated with 40 nm SiO_2 and 5 nm SiO_2 fluxes. The lowest values were measured after flux free TIG remelting. This trend corresponds well with the observed microstructural refinement, since finer dendritic structures and smaller dendritic colonies generally contribute to higher hardness [14]. Although the 40 nm SiO_2 flux produced the largest remelted area, the TiO_2 flux was more effective in refining the microstructure and increasing local hardness. Therefore, the results indicate that the flux composition affects the remelting process in two different ways: SiO_2 based fluxes, particularly 40 nm SiO_2, primarily increase the remelted zone size, while 20 nm TiO_2 provides the strongest microstructural refinement and hardness improvement.

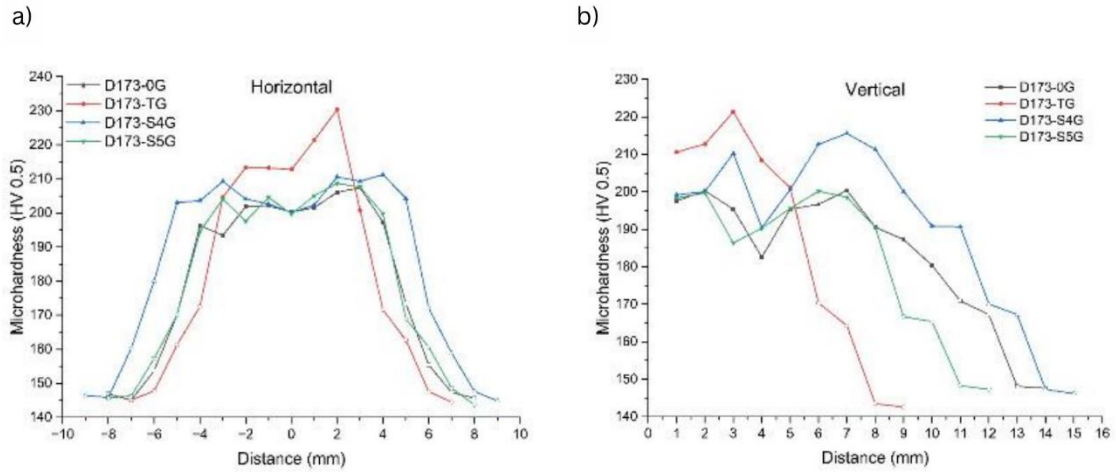


Figure 4. Microhardness profiles of ground PWAAM Al–Cu–Si deposits after 173 A DC TIG/ATIG remelting: (a) horizontal profiles measured 2 mm below the surface; (b) vertical profiles measured from the remelted surface towards the PWAAM-deposited material.

4. CONCLUSIONS

Based on the obtained results, the following conclusions can be drawn:

- TIG and activated TIG remelting at 173 A DC modified the near surface region of ground PWAAM Al–Cu–Si deposits, producing clearly defined remelted zones with increased microhardness compared with the surrounding additively manufactured material.
- The use of nanoparticle based activating fluxes affected the remelted zone geometry. The 40 nm SiO_2 flux produced the largest remelted zone, while the 5 nm SiO_2 flux also increased the remelted area compared with flux free TIG remelting.
- All investigated ground specimens exhibited relatively low porosity. However, retained Cu rich regions were still observed locally, particularly near the melt line or in the lower part of the remelted zone, indicating that complete dissolution of Cu rich particles was not achieved under all flux conditions.
- The flux composition also influenced the dendritic morphology and microhardness. The most pronounced microstructural refinement and the highest hardness were obtained with the 20 nm TiO_2 flux, followed by 40 nm SiO_2 and 5 nm SiO_2. Therefore, 40 nm SiO_2 was more effective for increasing the remelted zone size, while 20 nm TiO_2 was more effective for microstructural refinement and hardness improvement.

REFERENCES

[1] Williams, S. W., Martina, F., Addison, A. C., Ding, J., Pardal, G., Colegrove, P.: Wire + Arc Additive Manufacturing. Materials Science and Technology 32 (7), (2016), 641–647. DOI: 10.1179/1743284715Y.0000000073.

[2] Li, Y., Su, C., Zhu, J.: Comprehensive review of wire arc additive manufacturing: Hardware system, physical process, monitoring, property characterization, application and future prospects. Results in Engineering 13, (2022), 100330. DOI: 10.1016/j.rineng.2021.100330.

[3] Costello, S. C. A., Cunningham, C. R., Xu, F., Shokrani, A., Dhokia, V., Newman, S. T.: The state-of-the-art of wire arc directed energy deposition (WA-DED) as an additive manufacturing process for large metallic component manufacture. International Journal of Computer Integrated Manufacturing 36 (3), (2023), 469–510. DOI: 10.1080/0951192X.2022.2162597.

[4] Kim, J. T., Lee, S. W., Hong, S. H., Park, H. J., Park, J.-Y., Lee, N. S., Seo, Y., Wang, W.-M., Park, J. M., Kim, K. B.: Understanding the relationship between microstructure and mechanical properties of Al–Cu–Si ultrafine eutectic composites. Materials & Design 92, (2016), 1038–1045. DOI: 10.1016/j.matdes.2015.12.080.

[5] Park, J. M., Mattern, N., Kühn, U., Eckert, J., Kim, K. B., Kim, W. T., Chattopadhyay, K., Kim, D. H.: High-strength bulk Al-based bimodal ultrafine eutectic composite with enhanced plasticity. Journal of Materials Research 24 (8), (2009), 2605–2609. DOI: 10.1557/jmr.2009.0297.

[6] Park, J. M., Kim, K. B., Kim, D. H., Mattern, N., Li, R., Liu, G., Eckert, J.: Multi-phase Al-based ultrafine composite with multi-scale microstructure. Intermetallics 18 (10), (2010), 1829–1833. DOI: 10.1016/j.intermet.2010.02.042.

[7] Reisgen, U., Sharma, R., Oster, L.: Plasma Multiwire Technology with Alternating Wire Feed for Tailor-Made Material Properties in Wire and Arc Additive Manufacturing. Metals 9 (7), (2019), 745. DOI: 10.3390/met9070745.

[8] Kang, X., Li, G., Jiang, W., Li, F., Wang, Y., Wang, X., Zeng, Q., Fan, X.: Wire-Based Additive Manufacturing of Multi-Material Structures: A Review. Journal of Composites Science 9 (10), (2025), 534. DOI: 10.3390/jcs9100534.

[9] Jadhav, S., Kusekar, S., Belure, A., Digole, S., Mali, A., Cheepu, M., Mugale, M., Alkunte, S., Kim, D.: Recent Progress and Scientific Challenges in Wire-Arc Additive Manufacturing of Metallic Multi-Material Structures. Journal of Manufacturing and Materials Processing 9 (8), (2025), 284. DOI: 10.3390/jmmp9080284.

[10] Tashiro, S., Miyata, M., Tanaka, M.: Numerical analysis of AC tungsten inert gas welding of aluminum plate in consideration of oxide layer cleaning. Thin Solid Films 519 (20), (2011), 7025–7029. DOI: 10.1016/j.tsf.2011.04.137.

[11] Mannapovich, S. R., Touileb, K.: Improving the Formation and Quality of Weld Joints on Aluminium Alloys during TIG Welding Using Flux Backing Tape. Metals 14 (3), (2024), 321. DOI: 10.3390/met14030321.

[12] Sari, I., Ahmadein, M., Ataya, S., Hachani, L., Zaidat, K., Alrasheedi, N., Wu, M., Kharicha, A.: Prediction of the Secondary Arms Spacing Based on Dendrite Tip Kinetics and Cooling Rate. Materials 17 (4), (2024), 865. DOI: 10.3390/ma17040865.

[13] Kocjan, A., Logar, M., Shen, Z.: The agglomeration, coalescence and sliding of nanoparticles, leading to the rapid sintering of zirconia nanoceramics. Scientific Reports 7, (2017), 2541. DOI: 10.1038/s41598-017-02760-7.

[14] Rocha, O. L., Moreira, A. L., Costa, T. A., Filho, J. M. D., Paula, S. L., Silva, A. P.: Correlation between Thermal Parameters, Primary Dendrite Arm Spacing and Microhardness on a Directionally Solidified Ternary Al-6wt%Cu-8wt%Si Alloy. Defect and Diffusion Forum 365, (2015), 136–141. DOI: 10.4028/www.scientific.net/DDF.365.136